

# On-demand assembly of optically-levitated nanoparticle arrays in vacuum

Jiangwei Yan,<sup>1,2,\*</sup> Xudong Yu,<sup>1,2,\*</sup> Zheng Vitto Han,<sup>1,2</sup> Tongcang Li,<sup>3</sup> and Jing Zhang<sup>1,2,†</sup>

<sup>1</sup>*The State Key Laboratory of Quantum Optics and Quantum Optics Devices,  
Institute of Opto-Electronics, Shanxi University, Taiyuan 030006, China*

<sup>2</sup>*Collaborative Innovation Center of Extreme Optics,  
Shanxi University, Taiyuan, Shanxi 030006, China*

<sup>3</sup>*Department of Physics and Astronomy, Purdue University, West Lafayette, IN, USA*

(Dated: July 11, 2022)

Realizing a large-scale fully controllable quantum system is a challenging task in current physical research and has broad applications. Ultracold atom and molecule arrays in optical tweezers in vacuum have been used for quantum simulation, quantum metrology and quantum computing [1–5]. Recently, quantum ground state cooling of the center-of-mass motion of a single optically levitated nanoparticle in vacuum was demonstrated [6–8], providing unprecedented opportunities for studying macroscopic quantum mechanics [9–12] and precision measurements [13, 14]. In this work, we create a reconfigurable optically-levitated nanoparticle array in vacuum. Our optically-levitated nanoparticle array allows full control of individual nanoparticles to form an arbitrary pattern and detect their motion. As a concrete example, we choose two nanoparticles without rotation signals from an array to synthesize a nanodumbbell in-situ by merging them into one trap. The nanodumbbell synthesized in-situ can rotate beyond 1 GHz. Our work provides a new platform for studying macroscopic many-body physics [15–19] and quantum sensing [13, 14].

Optical levitation employs forces exerted by strongly focused light fields to capture and manipulate microparticles and nanoparticles [20–22]. As a result, an optically levitated system is naturally isolated from environmental disturbances. In particular, it possess extremely low damping in high vacuum and thus has an ultrahigh mechanical quality factor as an excellent optomechanical system. Hence, this system has attracted abroad attention and provides a powerful platform for precision measurements [13, 14] and fundamental physics investigations [9–12]. The center-of-mass (CoM) motion of an optically levitated nanoparticle has been cooled to the quantum ground state [6–8], and can be used to generate non-Gaussian macroscopic quantum states in future. Besides CoM motion, libration [23], rotation [24], and their coupling with internal degrees of freedoms (e.g., phonons, magnons, spin defects) of the levitated nanoparticle also provide rich physics to explore. In particular, the free rotation of a rigid body exhibits fascinating behaviors in both classical and quantum regimes due to its non-linear dynamics. We can now drive a single levitated nanoparticle to rotate at GHz frequencies [25–28], control its rotation with ultra-high precision [24, 29], and cool its librations to sub-kelvin temperatures [30, 31].

In this work, we report the creation, detection, and rearrangement of an array of optically levitated nanoparticles in vacuum. Ultracold atoms and molecules in an array of optical tweezers in vacuum have provide a versatile platform for large scale quantum simulation and quantum computing [1–5]. There are also significant progress in optical manipulation of multiple microparticles and

nanoparticles in a liquid [32–34]. However, creating a reconfigurable array of optically levitated nanoparticles in vacuum is still challenging due to the difficulty of loading multiple optical tweezers simultaneously and the lack of damping in vacuum to stabilize the system. Here we employ a high NA objective lens to tightly focus laser beams in the vertical direction against the gravity to create an array of optical tweezers. In this layout, the tightly focused optical tweezers provide large gradient forces for trapping and the gravity helps compensate the scattering force and photophoretic force to stabilize the system. As a result, our optical tweezers array can levitate silica nanoparticles at low pressures without feedback cooling. In addition, we use an independent detection laser beam to monitor the motion of each nanoparticle in the array. A control laser beam is used to move and rearrange nanoparticles to desired patterns. As an application of this technique, we choose two nanoparticles without rotational signals in an array to synthesize a silica nanodumbbell in-situ, and drive the created nanodumbbell to rotate at GHz frequencies. On-demand assembly of optically levitated nanoparticle arrays in vacuum will be important for creating macroscopic quantum entanglement [9–12] and studying complex phases of interacting systems [15–19].

The experimental protocol is illustrated in Fig. 1(a). A two-dimensional (2D) array of 1064 nm laser beams is created by a pair of orthogonal acousto-optic deflectors (AOD) driven by a multitone radio-frequency (RF) signal. The resulting beams are focused by a NA=0.95 objective lens to create an array of optical tweezers in a vacuum chamber. The optical tweezers propagate along vertical direction against the gravity. The power of each trapping beam is about 200 mW. More details can be found in Methods. Fig. 1(b) shows a simulated trapping

\* These authors contributed equally to this work

† Email: jzhang74@sxu.edu.cn, jzhang74@yahoo.com

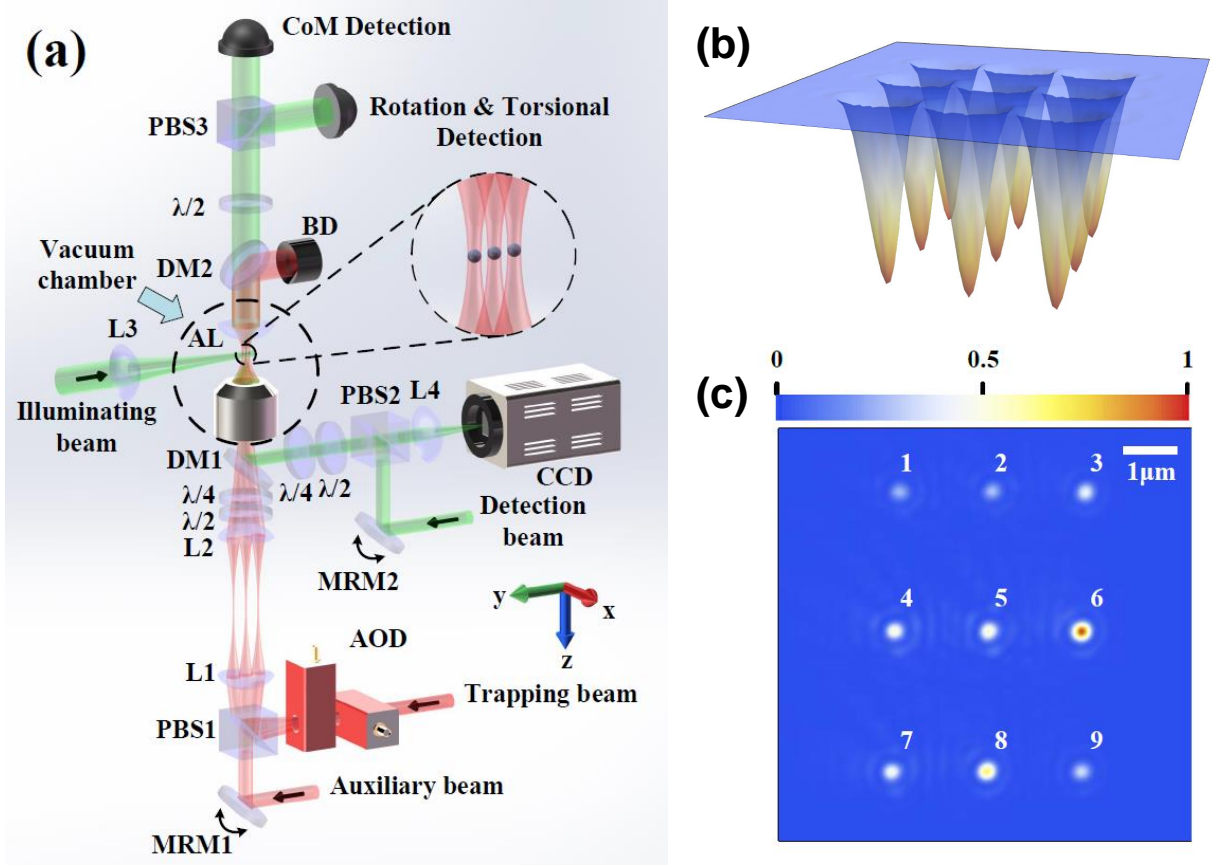


Figure 1. **Experimental setup and an image of an optically-levitated nanoparticle array.** (a) The 2D trap array is produced by passing a 1064 nm laser through a pair of orthogonal acousto-optic deflectors (AOD). The laser beams created by the AOD are imaged with a 4f image system onto a high NA ( $NA=0.95$ ) objective lens, which creates an array of tightly focused optical tweezers in a vacuum chamber. The optical tweezers propagate against gravity. For particle assembly, we use an auxiliary moving tweezer at 1064 nm superimposed on the trap array with a polarized beam splitter (PBS1). This auxiliary beam is deflected by a motor-driven reflective mirror (MRM1). For particle motion detection, we overlap a probe beam at 532 nm with the trapping beams using a dichroic mirror (DM1). This 532 nm beam is deflected by another motor-driven reflective mirror (MRM2) to measure the motion of an arbitrary particle in the array. The 1064 nm trap beams and the 532 nm probe beam after the high NA objective are collimated by an aspherical lens (AL) and separated by another dichroic mirror (DM2) for detecting the motion of trapped nanoparticles. For particle imaging, an imaging beam at 532 nm is used to illuminate the particles orthogonally. The scattered light is collected by the same high NA objective to form an image on an charge-coupled device (CCD).  $\lambda/2$ : half-wave plate; L1-4: spherical lens; BD: beam dump. (b) A simulated trapping potential of a  $3 \times 3$  two-dimensional (2D) array of optical tweezers. (c) An image of a  $3 \times 3$  array of optically levitated nanoparticles.

potential of a  $3 \times 3$  array of optical tweezers for single 170 nm nanoparticles. An auxiliary 1064 nm laser controlled by a motor-driven reflective mirror is used to rearrange nanoparticles into arbitrary patterns on demand. In addition, we use a 532 nm detection beam to measure the motion of trapped nanoparticles and a 532 nm illuminating beam for imaging. An photo of 9 nanoparticles trapped in an  $3 \times 3$  array is shown in Fig. 1(c). The horizontal distance of two adjacent columns is  $1.77 \mu\text{m}$  and the vertical distance of two adjacent rows is  $2.66 \mu\text{m}$ .

We can use the auxiliary trapping beam to rearrange the pattern of an array. By controlling the orientation of this laser, we can transport and remove the nanoparticles at the near atmospheric pressures with almost perfect success probabilities. Fig. 2 shows an example of such

on-demand rearrangement. First, we load the nanoparticles into a  $4 \times 4$  array of optical tweezers as shown in Fig. 2(a). We can see the initial filling of the array is probabilistic. Then we perform the rearrangement procedure to construct arbitrary and flexible patterns as shown in Fig. 2(b) and (c).

To exactly characterize each optically-levitated nanoparticle in the array, we use a probe beam to measure CoM and torsional motion of each nanoparticle. The CoM and torsional motion signals for each nanoparticle in an  $3 \times 3$  array [Fig. 1(c)] at 2000 Pa are shown in Fig. 3(a). We find that nanoparticles labeled as “1”, “2”, “3”, “7”, and “9” have no signal of torsional motion, which implicates these nanoparticles are near spherical. However, the nanoparticles labeled as

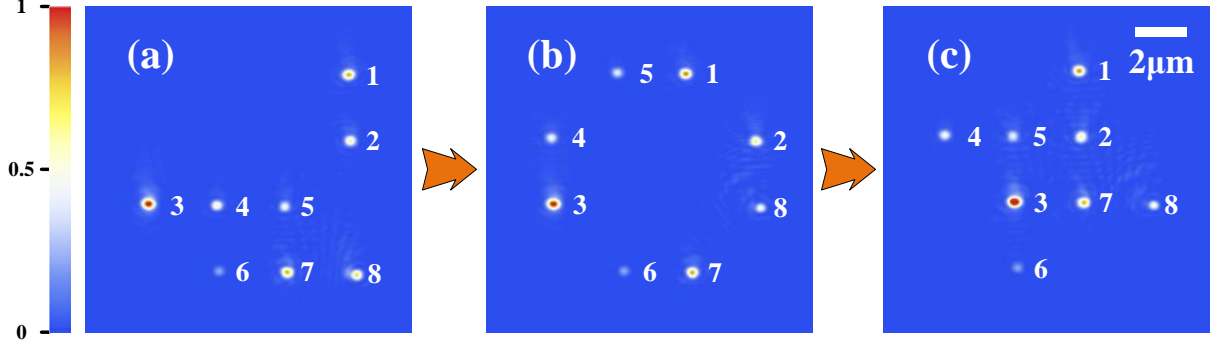


Figure 2. **Rearranging the pattern of a nanoparticle array.** (a) The initial pattern of 8 levitated nanoparticles in a  $4 \times 4$  array of optical tweezers. (b)-(c) Rearranged patterns of the nanoparticle array.

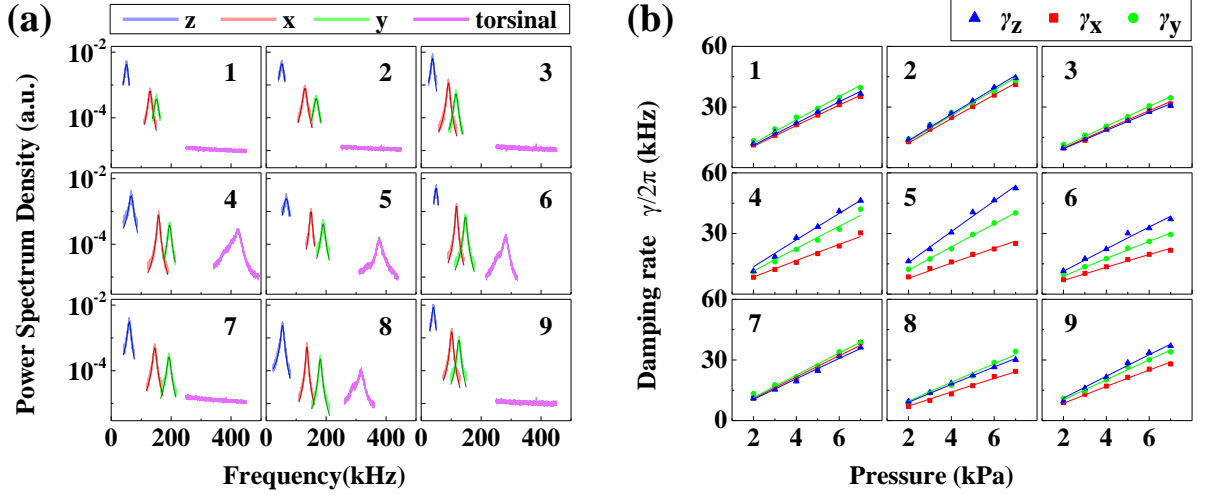


Figure 3. **Characterization of each nanoparticle in an optically-levitated nanoparticle array.** (a) The power spectra of the CoM and torsional motions for the  $3 \times 3$  trapped nanoparticles as shown in Fig. 1(c) at 2000 Pa. The blue, red, and green traces correspond to the power spectra of the CoM motions along the  $z$  axis,  $x$  axis, and  $y$  axis. The pink traces are the power spectra of torsional motions. (b) The damping rates of the CoM motions for the 9 trapped nanoparticles as a function of the pressure. The dots are measured data and the solid lines are linear fittings.

“4”, “5”, “6”, and “8” display torsional motion signals, indicating anisotropy in their shapes. Note that a linearly polarized trapping laser is used here to generate torsional motion of the trapped nanoparticle. We can model the nanoparticle as an ellipsoid with different sizes ( $r_1 > r_2 > r_3$ ) along three major axes. The longest axis with size  $r_1$  of the nanoparticle will tend to align with the electric field of the linearly polarized laser, which is defined as the  $x$  axis. This is because the polarizability of the nanoparticle along its longest size axis is the largest [26]. The trapping frequencies of the CoM motion depend on the polarization of the trapping laser [35]. The smaller radial trapping frequency is along the electric field of the linear polarized laser ( $x$  axis).

The damping rate  $\gamma_i$  of the CoM motion for a nanoparticle depends on the air pressure  $p$  and its shape ( $r_i$ ,  $i \in \{x, y, z\}$ ). It is proportional to  $p$  at low pressures

when the mean free path of air molecules is much larger than the size of the particle. A larger size in one direction will lead to a smaller damping rate of the CoM motion along that direction [26, 36]. Therefore, we can estimate the shape of the nanoparticle via the measured damping rates. Fig. 3(b) shows the damping rates of the CoM motion along three orthogonal directions as a function of the pressure. When the damping rates of the CoM motion along three orthogonal directions are almost the same (the curves labeled “1”, “2”, “3”, “7”, and “9” in Fig. 3(b)), we can infer that the shape of the nanoparticle is near spherical, which confirms the observation of no torsional signal for these nanoparticles. In contrast, the damping rate ratios  $\gamma_y/\gamma_x$  and  $\gamma_z/\gamma_x$  of CoM motion are large for “4”, “5”, “6”, and “8” nanoparticles, which means these nanoparticles are anisotropic. This agrees with the observation of torsional motion for these nanoparticles in a linearly polarized laser.

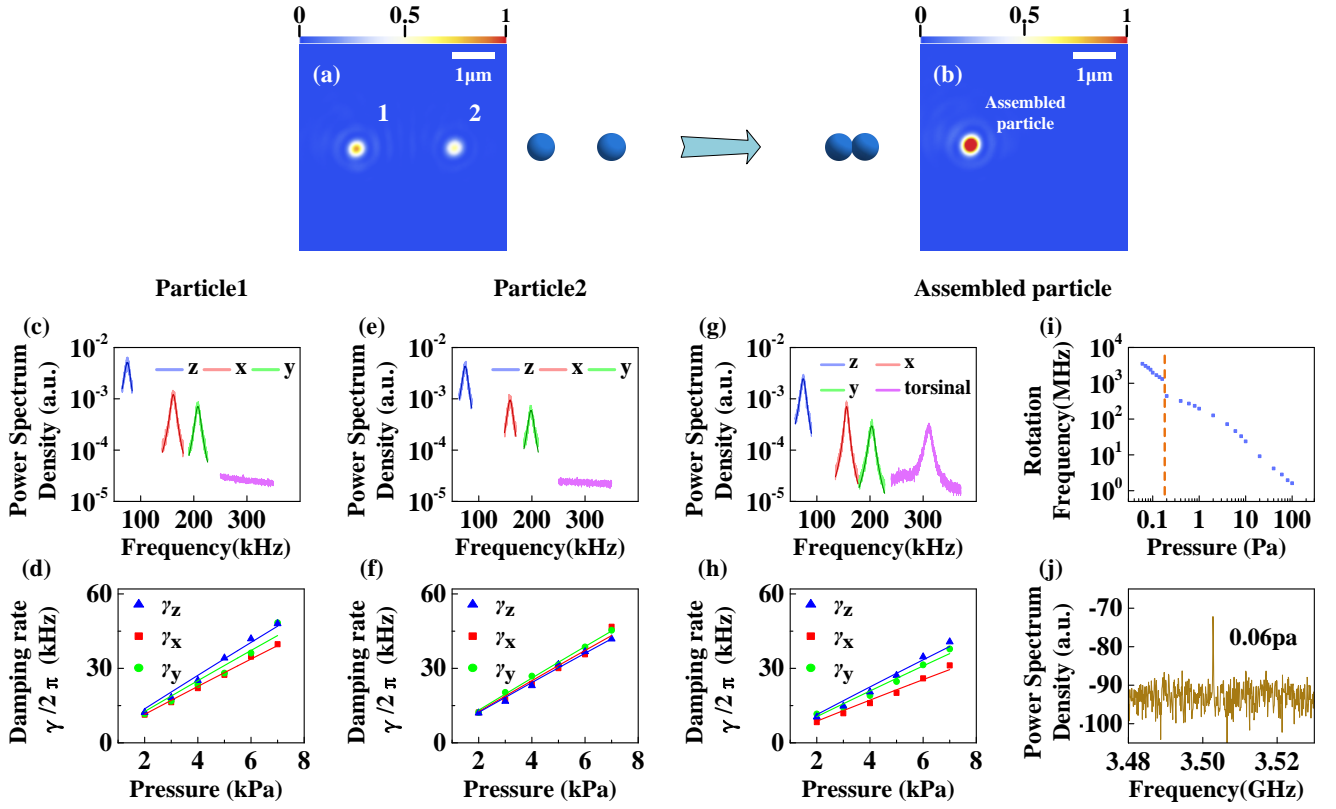


Figure 4. **In-situ synthesis of a nanodumbbell by merging two optically levitated nanoparticles.** (a) An image of two separated nanoparticles in two optical tweezers. (b) An image of the assembled nanoparticle. (c), (d) and (e), (f) CoM motion signals and the corresponding damping rates as functions of the pressures for nanoparticle 1 and 2 respectively. (g) and (h) CoM motion signals and the corresponding damping rates as a function of the pressure for the assembled nanodumbbell. For (c)-(h), the trapping laser beams are linearly polarized. (i) Rotational frequency of the nanodumbbell as a function of the pressure. (j) Rotational signal of the assembled nanodumbbell at 0.06 Pa. For (i) and (j), the trapping laser beam is circularly polarized.

After we obtain an optically-levitated nanoparticle array, we select two nanoparticles without torsional signals from the array to synthesize a nanodumbbell that supports fast rotation. Fig. 4(a) and (b) illustrate the assembling process. First we choose two nanoparticles from an array, which have no torsional motion signals as shown in Fig. 4(c)-(f). Then we control the auxiliary trapping beam to move one of two nanoparticles into the same trap. Two nanoparticles will stick together to become a nanodumbbell with 25% probability of success in a single trap. There are several other different situations for the two nanoparticles merged to a single trap. For example, the nanoparticles may be lost from the trap. The two nanoparticles may also remain separated in a trap, which may be due to the repulsive Coulomb force between them if they have the same sign of charges. These situations are discussed further in the supplementary material.

Figure 4(b) shows the image of the assembled nanodumbbell, whose intensity is larger than the individual nanoparticles. The CoM motion signals and the torsional motion signal are measured simultaneously, as shown in Fig. 4(g). There is almost no change in the trap-

ping frequencies of the CoM motion after assembly. The damping rates of the assembled nanodumbbell at different pressures are shown in Fig. 4(h). It shows a larger difference in damping rates for the CoM motion along three orthogonal directions and illustrates the anisotropic shape of the nanodumbbell. When we change the polarization of the trapping laser from linear to circular, the nanodumbbell is driven to rotate. The rotation frequency as a function of the pressure is shown in Fig. 4(i). A maximum rotation frequency of about 1.75 GHz at 0.06 Pa is observed (Fig. 4(j)). By further feedback cooling of CoM, the higher rotation frequency can be reached [28]

In conclusion, we have experimentally realized a 2D array of optically levitated nanoparticles in vacuum. The initial loading of the array is probabilistic, whereas the rearrangement procedure allows us to create defect-free arrays with high fidelity and construct flexible nanoparticle patterns on demand. By measuring the motion information, we can characterize each trapped nanoparticle, especially the anisotropic shape of the nanoparticle. As a solid application, we choose two nanoparticles without the rotational signals from the array to synthesize a nan-

odumbbell by moving the two nanoparticles into a trap. This work opens up a variety of opportunities, ranging from the assembly of complex systems with different types of nanoparticles to precision measurements [13, 14].

By applying cooling techniques [19] and utilizing optical binding [16–18], this system can be used to explore the many-body macroscopic quantum physics with interacting nanoparticles [9–12, 15].

- 
- [1] D. Barredo, S. de Léséleuc, V. Lienhard, T. Lahaye, and A. Browaeys, An atom-by-atom assembler of defect-free arbitrary two-dimensional atomic arrays, *Science* **354**, 1021 (2016).
  - [2] M. Endres, H. Bernien, A. Keesling, H. Levine, E. R. Anschuetz, A. Krajenbrink, C. Senko, V. Vuletic, M. Greiner, and M. D. Lukin, Atom-by-atom assembly of defect-free one-dimensional cold atom arrays, *Science* **354**, 1024 (2016).
  - [3] M. A. Norcia, A. W. Young, W. J. Eckner, E. Oelker, J. Ye, and A. M. Kaufman, Seconds-scale coherence on an optical clock transition in a tweezer array, *Science* **366**, 93 (2019).
  - [4] M. A. Norcia, A. W. Young, and A. M. Kaufman, Microscopic control and detection of ultracold strontium in optical-tweezer arrays, *Phys. Rev. X* **8**, 041054 (2018).
  - [5] L. Anderegg, L. W. Cheuk, Y. Bao, S. Burchesky, W. Ketterle, K.-K. Ni, and J. M. Doyle, An optical tweezer array of ultracold molecules, *Science* **365**, 1156 (2019).
  - [6] U. Delić, M. Reisenbauer, K. Dare, D. Grass, V. Vuletić, N. Kiesel, and M. Aspelmeyer, Cooling of a levitated nanoparticle to the motional quantum ground state, *Science* **367**, 892 (2020).
  - [7] L. Magrini, P. Rosenzweig, C. Bach, A. Deutschmann-Olek, S. G. Hofer, S. Hong, N. Kiesel, A. Kugi, and M. Aspelmeyer, Real-time optimal quantum control of mechanical motion at room temperature, *Nature* **595**, 373–377 (2021).
  - [8] F. Tebbenjohanns, M. L. Mattana, M. Rossi, M. Frimmer, and L. Novotny, Quantum control of a nanoparticle optically levitated in cryogenic free space, *Nature* **595**, 378–382 (2021).
  - [9] J. Li, I. M. Haghghi, N. Malossi, S. Zippilli, and D. Vitali, Generation and detection of large and robust entanglement between two different mechanical resonators in cavity optomechanics, *New Journal of Physics* **17**, 103037 (2015).
  - [10] J. Zhang, T. Zhang, and J. Li, Probing spontaneous wave-function collapse with entangled levitating nanospheres, *Phys. Rev. A* **95**, 012141 (2017).
  - [11] A. Bassi, K. Lochan, S. Satin, T. P. Singh, and H. Ulbricht, Models of wave-function collapse, underlying theories, and experimental tests, *Rev. Mod. Phys.* **85**, 471 (2013).
  - [12] T. Weiss and O. Romero-Isart, Quantum motional state tomography with nonquadratic potentials and neural networks, *Phys. Rev. Research* **1**, 033157 (2019).
  - [13] A. A. Geraci, S. B. Papp, and J. Kitching, Short-range force detection using optically cooled levitated microspheres, *Phys. Rev. Lett.* **105**, 101101 (2010).
  - [14] D. Carney, G. Krnjaic, D. C. Moore, C. A. Regal, G. Afek, S. Bhave, B. Brubaker, T. Corbitt, J. Cripe, N. Crisosto, A. Geraci, S. Ghosh, J. G. E. Harris, A. Hook, E. W. Kolb, J. Kunjummen, R. F. Lang, T. Li, T. Lin, Z. Liu, J. Lykken, L. Magrini, J. Manley, N. Matsumoto, A. Monte, F. Monteiro, T. Purdy, C. J. Riedel, R. Singh, S. Singh, K. Sinha, J. M. Taylor, J. Qin, D. J. Wilson, and Y. Zhao, Mechanical quantum sensing in the search for dark matter, *Quantum Science and Technology* **6**, 024002 (2021).
  - [15] S. Liu, Z.-q. Yin, and T. Li, Prethermalization and non-reciprocal phonon transport in a levitated optomechanical array, *Advanced Quantum Technologies* **3**, 1900099 (2020).
  - [16] Y. Arita, E. M. Wright, and K. Dholakia, Optical binding of two cooled micro-gyroscopes levitated in vacuum, *Optica* **5**, 910 (2018).
  - [17] V. Svak, J. Flajšmanová, L. Chvátal, M. Šiler, A. Jonáš, J. Ježek, S. H. Simpson, P. Zemánek, and O. Brzobohatý, Stochastic dynamics of optically bound matter levitated in vacuum, *Optica* **8**, 220 (2021).
  - [18] J. Rieser, M. A. Ciampini, H. Rudolph, N. Kiesel, K. Hornberger, B. A. Stickler, M. Aspelmeyer, and U. Delić, Observation of strong and tunable light-induced dipole-dipole interactions between optically levitated nanoparticles (2022).
  - [19] J. Vijayan, Z. Zhang, J. Piotrowski, D. Windey, F. van der Laan, M. Frimmer, and L. Novotny, Scalable all-optical cold damping of levitated nanoparticles (2022).
  - [20] Z.-Q. Yin, A. A. Geraci, and T. Li, Optomechanics of levitated dielectric particles, *Int. J. Mod. Phys. B* **27**, 1330018 (2013).
  - [21] J. Millen, T. S. Monteiro, R. Pettit, and A. N. Vamivakas, Optomechanics with levitated particles, *Rep. Prog. Phys.* **83**, 026401 (2020).
  - [22] C. Gonzalez-Ballester, M. Aspelmeyer, L. Novotny, R. Quidant, and O. Romero-Isart, Levitodynamics: Levitation and control of microscopic objects in vacuum, *Science* **374**, eabg3027 (2021).
  - [23] T. M. Hoang, Y. Ma, J. Ahn, J. Bang, F. Robicheaux, Z.-Q. Yin, and T. Li, Torsional optomechanics of a levitated nonspherical nanoparticle, *Phys. Rev. Lett.* **117**, 123604 (2016).
  - [24] F. Monteiro, S. Ghosh, E. C. van Assendelft, and D. C. Moore, Optical rotation of levitated spheres in high vacuum, *Phys. Rev. A* **97**, 051802 (2018).
  - [25] R. Reimann, M. Doderer, E. Hebestreit, R. Diehl, M. Frimmer, D. Windey, F. Tebbenjohanns, and L. Novotny, Ghz rotation of an optically trapped nanoparticle in vacuum, *Phys. Rev. Lett.* **121**, 033602 (2018).
  - [26] J. Ahn, Z. Xu, J. Bang, Y.-H. Deng, T. M. Hoang, Q. Han, R.-M. Ma, and T. Li, Optically levitated nanodumbbell torsion balance and ghz nanomechanical rotor, *Phys. Rev. Lett.* **121**, 033603 (2018).
  - [27] J. Ahn, Z. Xu, J. Bang, P. Ju, X. Gao, and T. Li, Ultrasensitive torque detection with an optically levitated nanorotor, *Nat. Nanotechnol.* **15**, 89 (2020).

- [28] Y. Jin, J. Yan, S. J. Rahman, J. Li, X. Yu, and J. Zhang, 6 ghz hyperfast rotation of an optically levitated nanoparticle in vacuum, *Photon. Res.* **9**, 1344 (2021).
- [29] S. Kuhn, A. Kosloff, B. A. Stickler, F. Patolsky, K. Hornberger, M. Arndt, and J. Millen, Full rotational control of levitated silicon nanorods, *Optica* **4**, 356 (2017).
- [30] J. Bang, T. Sebersson, P. Ju, J. Ahn, Z. Xu, X. Gao, F. Robicheaux, and T. Li, Five-dimensional cooling and nonlinear dynamics of an optically levitated nanodumbbell, *Phys. Rev. Research* **2**, 043054 (2020).
- [31] F. van der Laan, F. Tebbenjohanns, R. Reimann, J. Vijayan, L. Novotny, and M. Frimmer, Sub-kelvin feedback cooling and heating dynamics of an optically levitated librator, *Phys. Rev. Lett.* **127**, 123605 (2021).
- [32] K. Sasaki, M. Koshioka, H. Misawa, N. Kitamura, and H. Masuhara, Pattern formation and flow control of fine particles by laser-scanning micromanipulation, *Opt. Lett.* **16**, 1463 (1991).
- [33] E. R. Dufresne, G. C. Spalding, M. T. Dearing, S. A. Sheets, and D. G. Grier, Computer-generated holographic optical tweezer arrays, *Review of Scientific Instruments* **72**, 1810 (2001), <https://aip.scitation.org/doi/pdf/10.1063/1.1344176>.
- [34] M. P. MacDonald, L. Paterson, K. Volke-Sepulveda, J. Arlt, W. Sibbett, and K. Dholakia, Creation and manipulation of three-dimensional optically trapped structures, *Science* **296**, 1101 (2002), <https://www.science.org/doi/pdf/10.1126/science.1069571>.
- [35] Y. Jin, X. Yu, and J. Zhang, Polarization-dependent center-of-mass motion of an optically levitated nanosphere, *J. Opt. Soc. Am. B* **36**, 2369 (2019).
- [36] Y. Jin, X. Yu, and J. Zhang, Optically levitated nanosphere with high trapping frequency, *Sci. China Phys. Mech. Astron.* **61**, 114221 (2018).
- [37] Y. Jin, J. Yan, S. J. Rahman, X. Yu, and J. Zhang, Imaging the dipole scattering of an optically levitated dielectric nanoparticle, *Applied Physics Letters* **119**, 021106 (2021), <https://doi.org/10.1063/5.0053008>.
- [38] Y. Jin, J. Yan, S. J. Rahman, X. Yu, and J. Zhang, Interference of the scattered vector light fields from two optically levitated nanoparticles, *Opt. Express* **30**, 20026 (2022).

## METHODS

Our scheme to create an optically levitated nanoparticle array in vacuum is shown in Fig. 1 in the main text. A 2D laser beam array is created by passing a 1064 nm laser through a pair of orthogonal acousto-optic deflectors (AOD) driven by a multitone radio-frequency (RF) signal. The resulting beam array is imaged with a 1:1 telescope onto a high NA ( $NA=0.95$ ) objective lens, which creates an array of tightly focused optical tweezers in a vacuum chamber. An auxiliary 1064 nm laser with the orthogonal linear polarization is combined with the trapping beam array with a polarizing beam splitter (PBS1) and focused by the same objective. The orien-

tation of this beam is controlled by a motor-driven reflective mirror to rearrange nanoparticles trapped by the optical tweezers array into any patterns. In order to obtain motion information of the trapped nanoparticles, a 532 nm probe beam is combined with the trapping beams by a dichroic mirror (DM1) before the vacuum chamber. The orientation of this 532 nm beam can be adjusted to make it focus on an arbitrary particle in the array. The strongly focused 1064 nm trapping laser beams and the 532 nm probe beam are collimated by an aspherical lens with  $NA=0.78$ . The output 532 nm laser and 1064 nm laser beams from the vacuum chamber are separated by another dichroic mirror (DM2). The 532 nm probe beam is then split into two parts for detecting the center-of-mass (CoM) motion, and rotation or torsional motion of trapped nanoparticles. When measure the high-speed rotation at low pressure, we directly use the 1064 nm trapping laser to detection the rotation signal.

Commercial silica nanoparticles with a nominal diameter of 170 nm are utilized. The monodisperse nanoparticles are dispersed into the vacuum chamber by an ultrasonic nebulizer and trapped by the optical tweezer array with each beam at about 200 mW. In order to image the optically-levitated nanoparticle array, another 532 nm beam is used to illuminate those particles orthogonal to the optical axis of the high NA objective lens. The scattering light is collected by the same high NA objective to form an image on a charge-coupled device (CCD). This configuration provides a dark background and a high signal-noise ratio for imaging levitated nanoparticles [37, 38]. The scattering 532 nm light intensity shown in the image provides preliminary information about the size of each trapped nanoparticle. The spatial distance among the nanoparticles can be precisely measured according to the interference fringes of the scattered 532 nm lights from the particles. After the loading procedure, we start a vacuum pump to evacuate air from the vacuum chamber.

## CODE AVAILABILITY

The custom codes that support the findings of this study are available from the corresponding author upon reasonable request.

## ACKNOWLEDGMENTS

This research was supported in part by National Natural Science Foundation of China (NSFC) (Grant No. 61975101, 11234008, 11361161002, 61571276).

## AUTHOR CONTRIBUTIONS

J.Z. designed and supervised the project. J.Y., X.Y. and J.Z. performed the experiments. All authors anal-

ysed the data and discussed the results. J.Z., J.Y., and T.L. wrote the manuscript. All authors interpreted the results and reviewed the manuscript.